JOURNAL OF MATERIALS SCIENCE 30 (1995) 3576–3586

Strain-rate and grain-size effect on substructures and mechanical properties in OFHC copper during tension

H. SHANKARANARAYAN, S. K. VARMA
Department of Metallurgical and Materials Engineering, The University of Texas at El Paso, El Paso, Texas 77968, USA

The combined effect of grain size (recrystallized grains of 34, 86, 105 and 128 μm) and strain rate (0.01, 0.05, 0.25, 2.5 and 5 min^{-1}) on the evolution of dislocation substructures and mechanical properties in oxygen-free high conductivity (OFHC) copper during room-temperature tensile testing has been studied. Under identical conditions of deformation, the flow stress values for smaller grain size were higher than those for larger grain sizes with the exception in the case of 86 μm which has been attributed to the inhomogeneous substructural developments in the microstructures. The cell size decreases monotonically with increase in per cent strain indicating no signs of cell size saturation. The effect of strain rate on the development of dislocation substructures at constant strain is such that the cell size decreases initially but increases with further increase in strain rate for smaller grain sizes of 34 and 86 μm while a reverse trend has been observed for larger grain sizes of 105 and 128 μm. A graph of the cell size strengthening coefficient, *k*, and the strain rate shows three distinct stages in the curves for different grain sizes.

1. Introduction

The rate at which the metals can be deformed (strain rate) influences the production rate for most of the metal-forming operations, e.g. rolling, wire drawing, etc. Even though the individual effects of grain size and strain rate on the mechanical properties may be somewhat understood, their combined effect on microstructural developments and mechanical properties is relatively unknown, especially towards the low strain-rate regime (the low and high strain-rate regimes correspond to the strain-rate values of less or greater than 10^3 s^{-1}, respectively).

1.1. Substructure formation

Holt [1] pointed out that a uniformly dense dislocation distribution is unstable against fluctuations in their density, because the elastic energy of the system can be reduced by clustering. This clustering of dislocations results in the formation of cells and the cell size is determined by the distance at which the elastic stress between the cell walls becomes too small to affect the motion of other dislocations. The evidence of dislocation cell structure in heavily drawn copper was first reported by Embury *et al.* [2]. Chevel and Priester [3] have shown that under dynamic loading, well-defined cell structure is not observed in polycrystalline copper whereas it was observed during static deformation.

According to Kuhlmann–Wilsdorf's mesh length theory [4] the flow stress, σ, is directly proportional to the square root of the dislocation density, ρ,

$$\sigma = \sigma_0 + \alpha G\boldsymbol{b}(\rho)^{1/2} \quad (1)$$

where σ_0 is the frictional stress, α is a constant, G is the shear modulus and $\boldsymbol{b}$ is the Burgers vector. Coarse and irregular cells with thick boundaries at low strains were reported by Malin and Heatherly [5] and the cell diameter, d, was found to be inversely proportional to the square root of the dislocation density by Staker and Holt [6] and Kocks and Mecking [7] in copper

$$d = K(\rho)^{-1/2} \quad (2)$$

where K is a constant. Combining Equations 1 and 2 we obtain

$$\sigma = \sigma_0 + K\alpha G\boldsymbol{b}(d)^{-1} \quad (3)$$

This equation shows that the flow stress is inversly related to the cell diameter. According to Kocks and Mecking [7] the kinetics of plastic flow are determined by a single structure parameter, the total dislocation density, which is in turn related to the cell size according to Equation 2. Knoeson and Kritzinger [8] and Lan *et al.* [9] have proposed that the decrease in cell diameter during the deformation in iron is caused by the formation of new cells or macroscopic shape change. Carson and Weertman [10] have reported that up to 10% strain, the dislocations interact with each other to form tangles and, with increase in strain, the tangles link together to form cells. However, with increase in strain during the deformation the individual cells continue to rotate relative to each other and this becomes increasingly more difficult for a deforming cell block with the same combination of slip systems and hence the blocks are expected to decrease in size according to Hansen [11]

0022–2461

Park and Parker [12] have shown that the microbands are formed at high strain rates and high temperature also favours the formation of inhomogeneous microstructures in the form of microbands. But Nix and Hughes [13] found that the tendency to form microbands decreased at higher temperatures in nickel. The band structure consists of high dislocation density in the walls while the interior of the band is relatively free of dislocations. Hensen and Hanson [14] have noted that for small and medium grain sizes the microbands have a tendency to extend from one grain boundary to another, whereas microbands stop in the interior of the large grains. Most of the theories explaining the formation of microbands describe them as a consequence of strain inhomogeneity during the deformation. According to Tome *et al.* [15] microbands are formed due to microscopic shear, while Ananthan *et al.* [16] have reported the formation of second generation microbands in cold-rolled copper. They observed that the second generation microbands formed at larger strains (> 20%) carried a greater fraction of shear strain compared to that carried by the first generation microbands.

TABLE I Spectrometric analysis of OFHC copper (atomic parts per million by weight)

O	C	Fe	Ag	Sb	Pb	S	As	N	Si
22	9.0	1.5	1.2	0.73	0.7	0.68	0.64	8	0.38

TABLE II Annealing schedule

Rod diameter (mm)	Temperature (°C)	Time (h)	Grain diameter (μm)
3.66	550	1.25	34
4.11	600	1.25	86
6.53	650	4.0	105
8.23	750	6.0	128

1.2. Effect of grain size

The grain size is one of the most important parameters which affects the strength of a material. Fine-grained materials have higher dislocation density than coarse-grained materials and therefore have higher strengths. Thompson *et al.* [17] have described the grain-size dependence of the limiting slip-length (cell-size) decreases with a decrease in the stacking fault energy (SFE) values. Thompson [18] has shown, in deformed

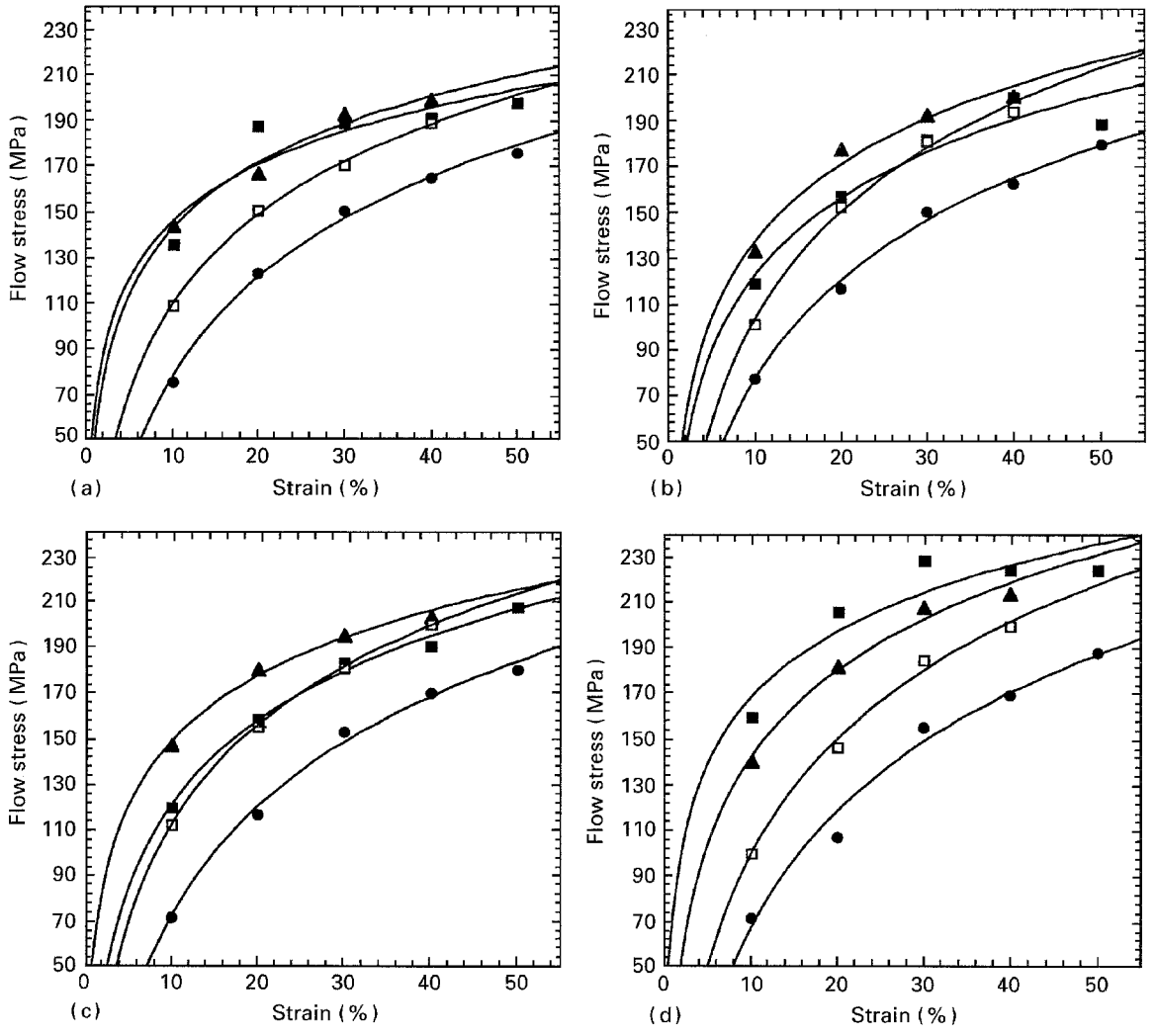

Figure 1 Flow stress–percent strain curves for OFHC copper rods deformed in tension for four grain sizes of (▲) 34, (■) 86, (□) 105, and (●) 128 μm at strain rates of (a) 0.01, (b) 0.05, (c) 0.25 and (d) 2.5 min^{-1}.

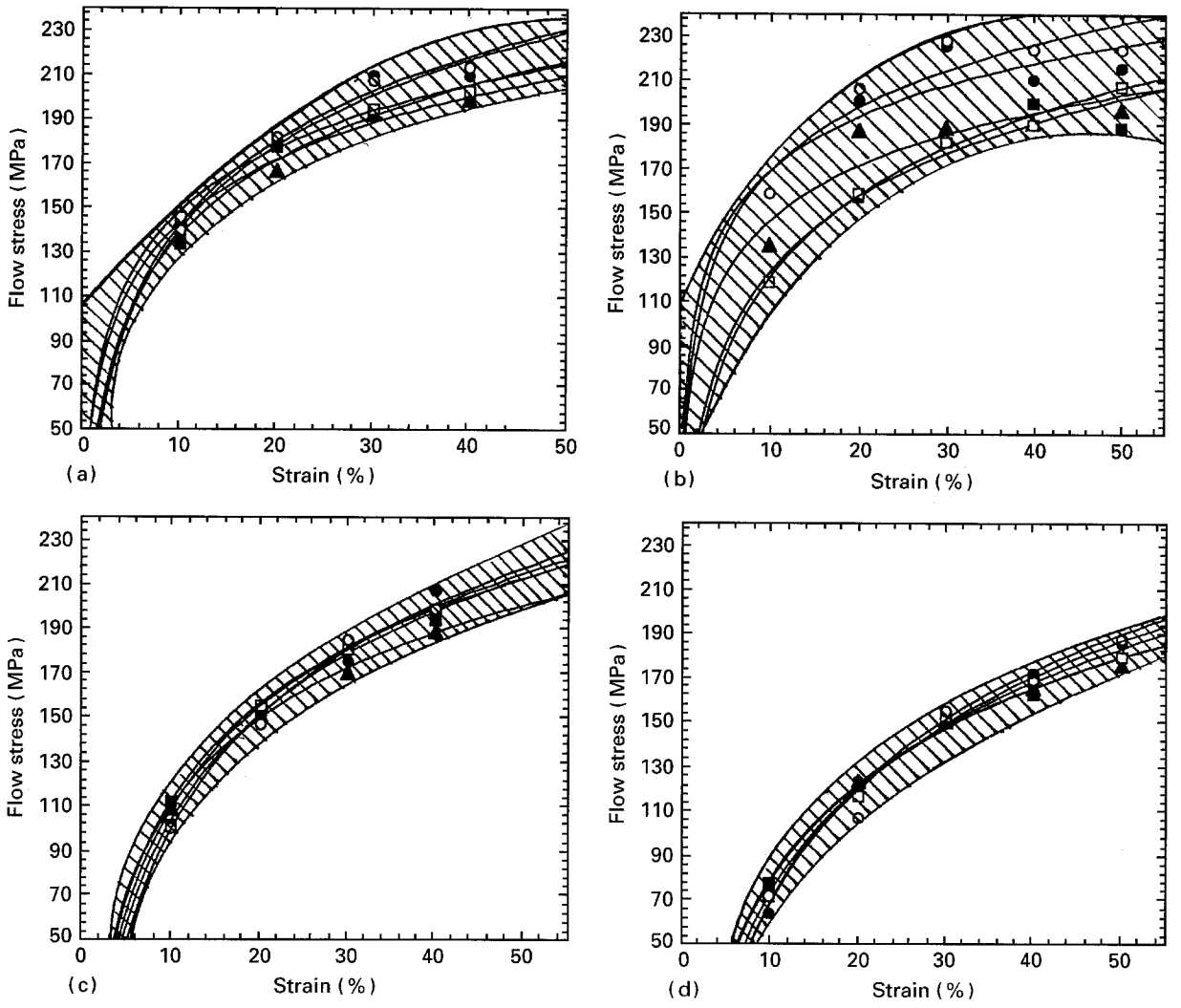

Figure 2 Flow stress–percent strain curves at four different strain rates of (▲) 0.01, (■) 0.05, (□) 0.25, (●) 2.5 and (○) 5 min^{-1} for the grain sizes of (a) 34, (b) 86, (c) 105 and (d) 128 μm.

copper with a grain size of 3.4 μm, that cells were fragmented and poorly formed even at a high strain of 0.3, whereas in larger grains, cells were sharp at this strain.

Parry and Walker [19] have indicated the bilinear nature of the Hall–Petch plot. They attribute this behaviour to the fact that influence of grain boundaries is decreased at strain values above 1% by the

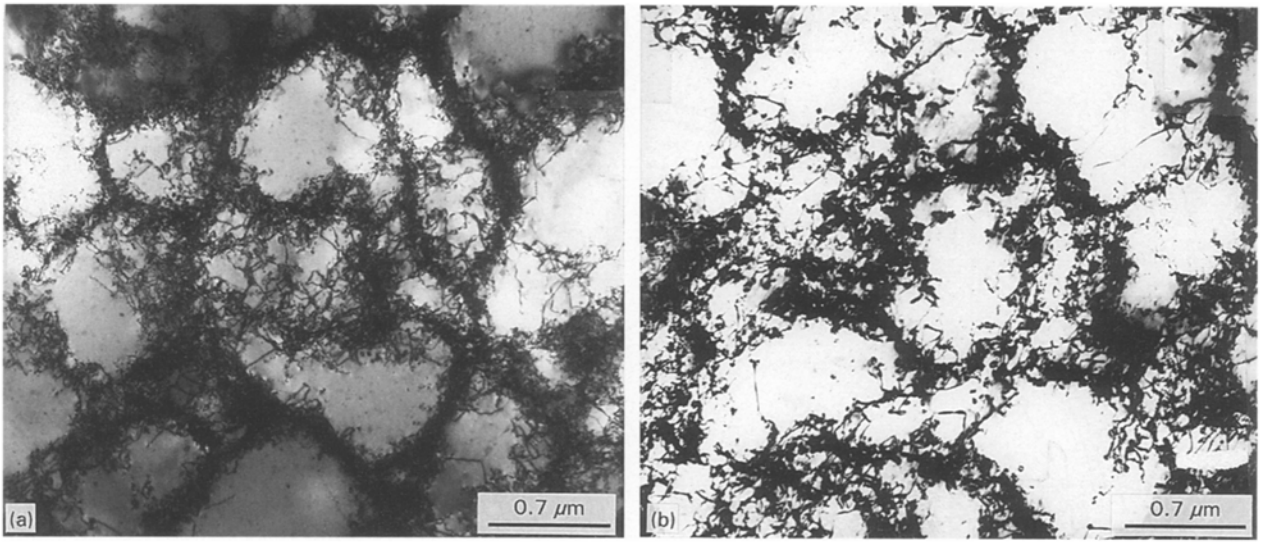

Figure 3 Comparison of microstructural evolution at a strain rate of 0.01 min^{-1} and a strain of 20% between four different grain sizes: (a) 34, (b) 86, (c) 105 and (d) 128 μm.

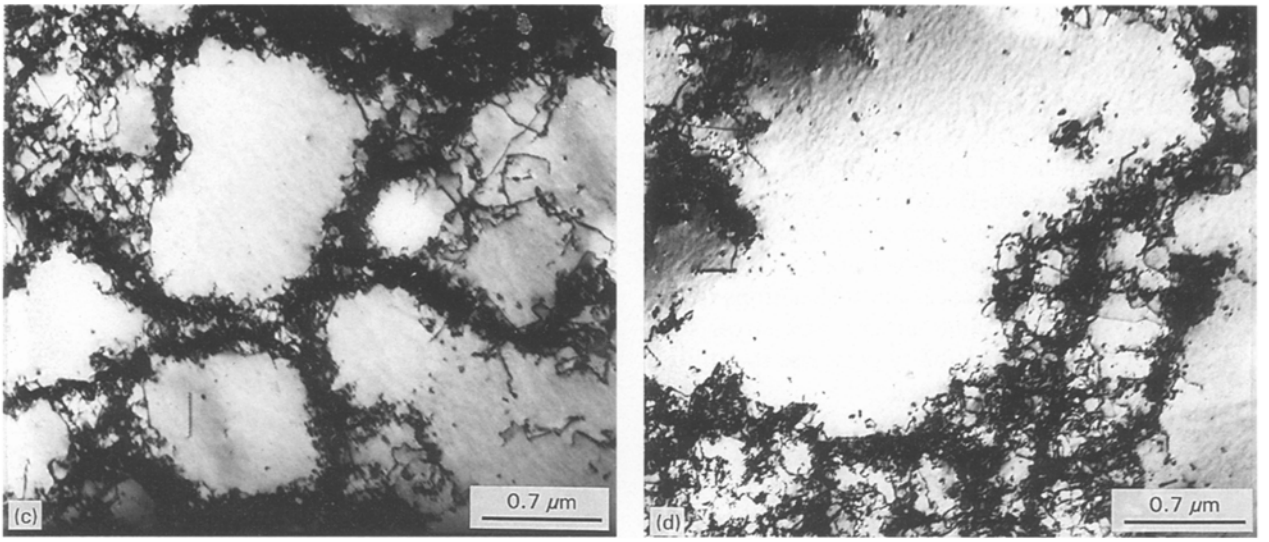

Figure 3 (Continued).

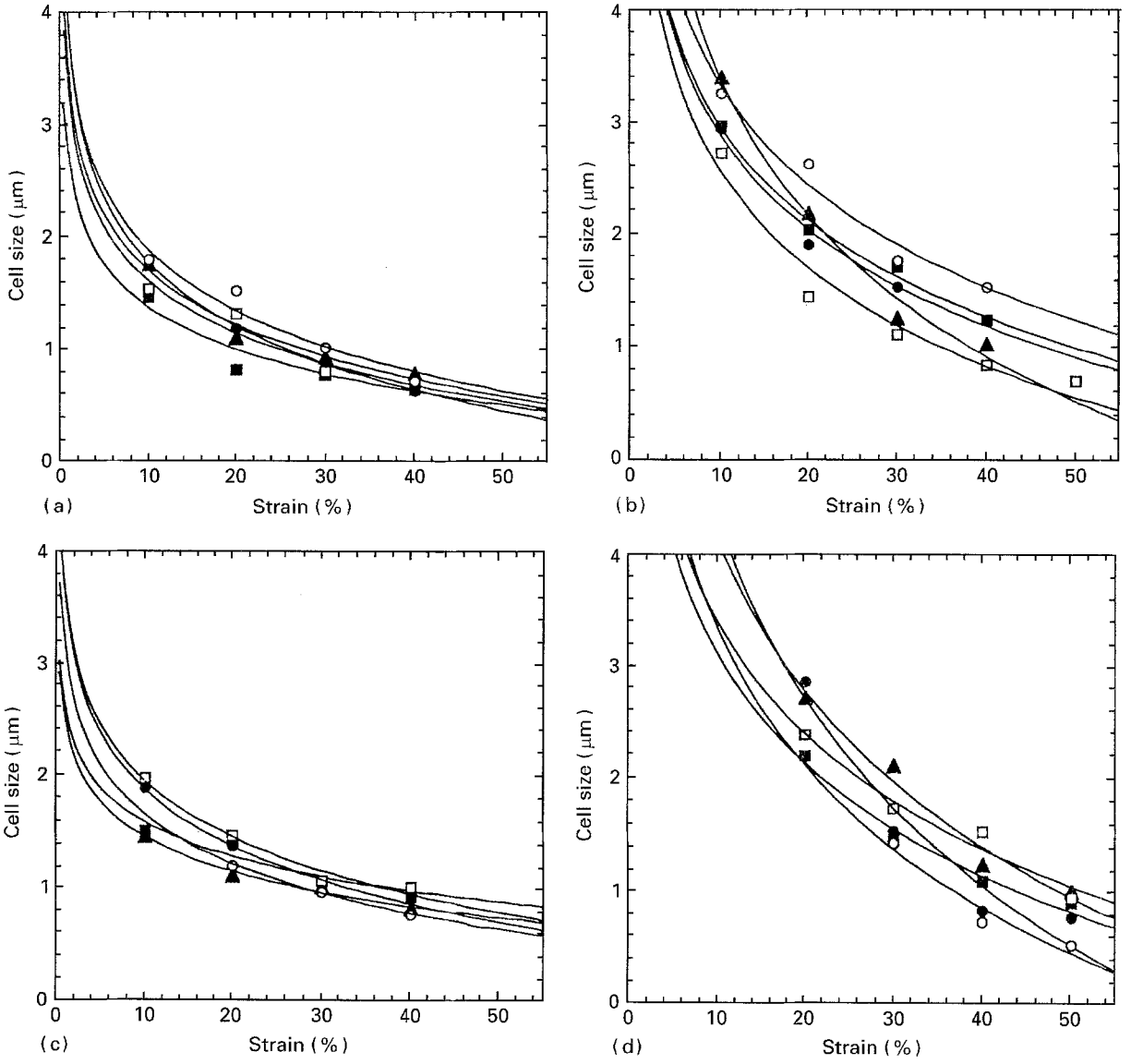

Figure 4 Variation of cell size as a function of percent strain at five different strain rates of (▲) 0.01, (■) 0.05, (□) 0.25, (●) 2.5 and (○) 5 min^{-1} for the grain sizes of (a) 34, (b) 86, (c) 105 and (d) 128 μm.

formation of dislocation substructures (cells) within the grains; this has been confirmed in nickel by Mehta and Varma [20]. Fujita and Tabata [21] have shown discontinuity of the Hall–Petch relationship, in order to describe the grain-size strengthening, in polycrystalline aluminium. They attribute this to the mean spacing of the barriers for active dislocations being influenced by obstacles such as cell walls, subgrain

boundaries, etc. Therefore, the grain size in the Hall–Petch relation should be replaced by the mean free path of the dislocations.

Gracio and Fernandes [22] have shown, in copper, that for larger grain sizes, parallel walls of dislocations are formed with the (1 1 1) plane, the principal active slip plane trace. For smaller grain sizes, two families of dislocation walls crossing each other lead to a closed cell. They have shown for smaller grain sizes that the density of geometrically necessary dislocations reduces the initial cell size, and the complex stress state required by strain compatibility gives rise to multiple slip which leads to a closed cell.

Gourdin and Lassila [23] have demonstrated in polycrystalline copper that larger grains show more heterogeneous deformation than smaller grains while subdivisions are also pronounced in larger grains. Microbands which form the heterogeneous microstructure are reduced in fine-grained aluminium whereas well-developed microbands are observed in medium- and large-grained specimens. For tensile strained copper [22], it has been found that only one family of walls is formed in large-grained specimens, while two intersecting sets of walls are found in small- to medium-grained specimens.

Dingley and McLean [24] have shown that the flow stress is a unique function of dislocation density, irrespective of grain size in bcc metals. Even though smaller grain size has higher dislocation density than larger grain size, too small a grain size can actually hinder the cell formation, as shown by Thompson [25] in nickel. The strength of a material can be increased by refining the microstructure, i.e. by reducing the grain size. However, research has shown that there is a limit to the strength that can be increased by grain-size refinement [26].

1.3. Effect of strain rate

Korbel and Swiatkowski [27] have found the thermally activated relaxation processes, which reduce the internal stress causing the softening, to be time dependent. Thus the plastic deformation at higher strain rates should reduce the relaxation process and result in higher flow stress. Gourdin and Lassila [23] have shown that for a given strain rate, the hardening of OFHC copper at a fixed strain rate is independent of the grain size in a range from 10–200 μm. The Thiagarajan and Varma group [28–31] has shown that the rate of cell-size refinement with respect to tensile strain decreases with increase in strain rate, and cell-size strengthening as a function of strain rate is more effective at lower tensile strains in copper. Sil and co-workers [32–34] have shown that the cell boundaries are well defined at lower strain rates in aluminium and nickel compared to those formed at higher strain rates. Murr and Kuhlmann-Wilsdorf [35] have observed that cells formed are less well defined after shock loading compared to cells formed at low strain rates in nickel. Gurevitch *et al.* [30] showed no cell formation during shaped charge jet formation because of dynamic recrystallization. Parry and Walker [19] have shown that for strain rates up to $10^3\ s^{-1}$ there exists a linear relationship between the flow stress and log of strain rate at a given strain and grain size. Above the strain rate of $10^3\ s^{-1}$ the stress at a given strain increases rapidly with strain rate. Rao and Varma [34] have shown that there is

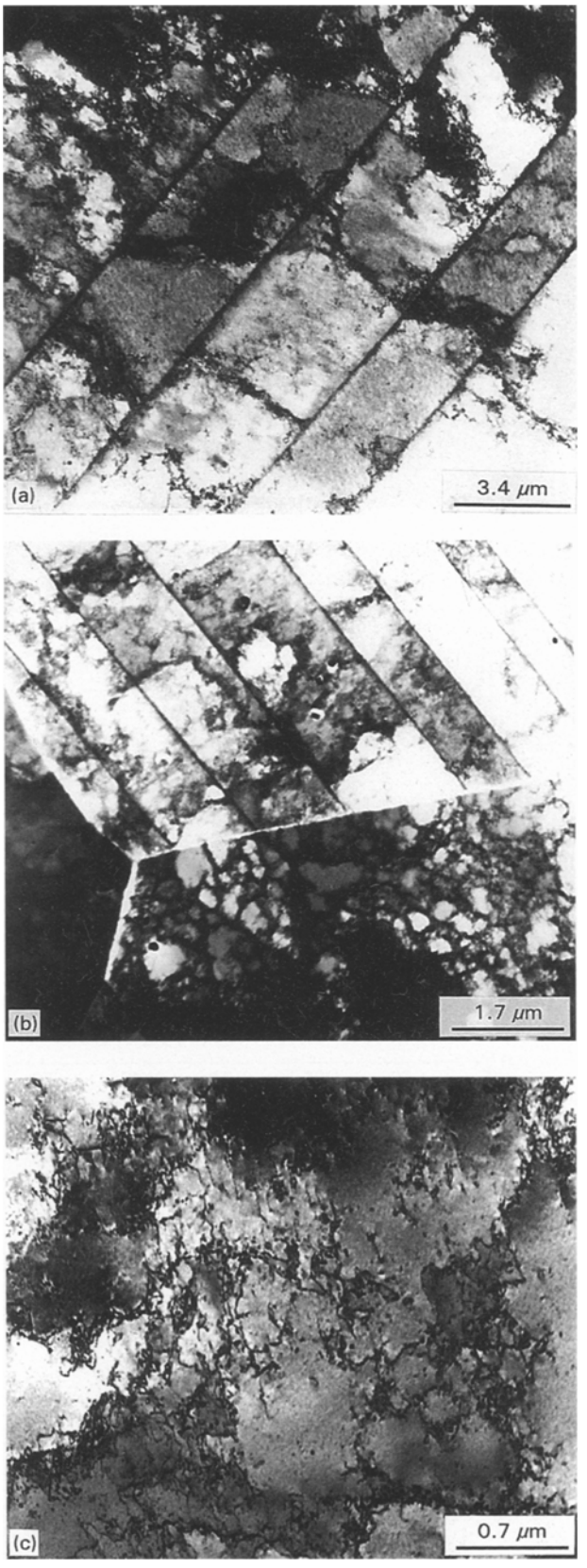

Figure 5 Micrographs showing inhomogeneity in the microstructure for the grain size of 86 μm deformed to 10% strain at a strain rate of 5 min^{-1}. The three micrographs are from within a single foil.

a cell-size saturation that takes place at lower strain rates during tensile testing while higher strain rates do not reach this stage.

This paper presents the results of a study on the combined effect of grain size and strain rate on the development of dislocation substructures and flow stresses during tensile testing at room temperature in OFHC copper.

2. Experimental procedure

The spark spectrometric analysis in atomic parts per million by weight of the OFHC copper used in this study is shown in Table I.

The cold-drawn rods of different diameters were annealed at various combinations of time and temperature to obtain grain diameters of 34, 86, 105 and 128 μm as shown in Table II.

The grain-size measurements were made on the short cross-sections of the rods by using standard techniques of optical metallography. The etching was done using a mixture consisting of equal volumetric ratios of phosphoric acid, glacial acetic acid and nitric acid. The grain size was determined by the linear intercept method by counting at least 500 grains and multiplying the intercept length by the shape factor of 1.68 to convert them to grain diameters.

The annealed samples were subjected to tensile testing to engineering strains of 10%, 20%, 30% and 40% at different strain rates of 0.01, 0.05, 0.25, 2.5 and 5 min^{-1} using an Instron 1127 machine. The gauge lengths of the samples were kept at 5.08 cm and the strain rates were calculated by dividing the crosshead speeds with the gauge length.

Thin transverse wafers were cut from the tensile-tested samples with Buehler Isomet cutting machine at low speeds using a diamond saw and appropriate lubricant. These wafers were mechanically ground to a thickness of 0.3 mm and discs of 3 mm diameter were punched using a hand punch. The wafers were then electropolished using a Tenupol-3 electropolisher with the following conditions: (a) electrolyte–distilled water (1100 ml), phosphoric acid (400 ml), ethanol (500 ml), Vogel's sparbeieze (a special solution developed by the Struer's Company, 4 ml) and propanol (10 ml), (b) temperature, 2 °C, (c) flow rate setting 3.5, (d) voltage,

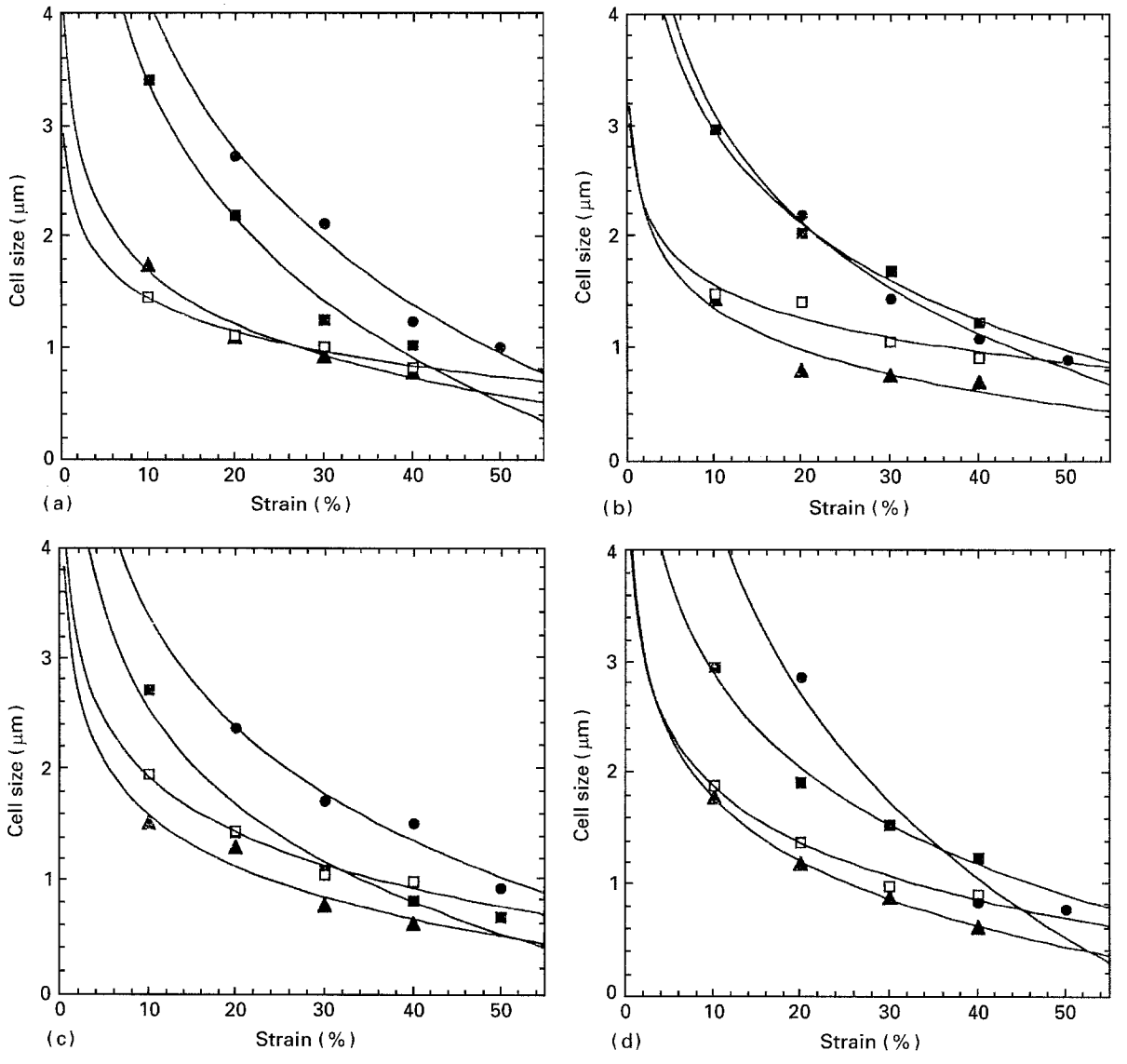

Figure 6 Variation of cell size as a function of percent strain for four different grain sizes of (▲) 34, (■) 86, (□) 105 and (●) 128 μm at strain rates of (a) 0.01, (b) 0.05, (c) 0.25 and (d) 2.5 min^{-1}.

5 V, and (e) current 0.06–0.09 A. An Hitachi H-8000 scanning transmission electron microscope (STEM) was used at 200 kV to observe the microstructures. At least nine different foils were observed for a given deformational condition. The cell diameters were measured using the linear intercept method as explained for the grain-size measurement. At least 500 cell-wall intercepts with the test line were counted to calculate the cell diameter.

3. Results and discussion

Fig. 1 shows the effect of per cent strain on the flow stress in OFHC copper during tensile testing at room temperature for different grain sizes of 34, 86, 105 and 128 μm. The four graphs correspond to four different strain rates of 0.01, 0.05, 0.25, and 5 min^{-1}. It must be noted that the graphs do not represent the conventional stress–strain curves in this figure. The samples of a particular grain size were deformed to a specified amount of engineering strain at a fixed strain rate and the flow stress was recorded. The experiments were repeated for different engineering strain values and a curve is obtained in one of these graphs. The procedure was repeated for other three grain sizes and strain rates. In general, within the limits of experimental scatter in the data, Fig. 1 clearly demonstrates the grain-size strengthening in OFHC copper and also confirms that increasing the strain rate increases the flow stress values.

One of the interesting features of Fig. 1 can be more easily recognized if the data are plotted for different grain sizes instead of different strain rates, as shown in Fig. 2. With the exception of 86 μm grain size, the flow stress values become insensitive to the changes in strain rate as the grain sizes increases. This has been shown for aluminium [33], nickel [34] and 304 stainless steel [36] also. Obviously the trend could be verified by determining the strain-rate sensitivity in single crystals.

The qualitative analysis of the microstructural developments taking place in OFHC copper during room-temperature tensile testing is shown in Fig. 3. It shows a typical example of the microstructural evolution when copper of this study is deformed to a strain of 20% at a strain rate of 0.01 min^{-1} for four different

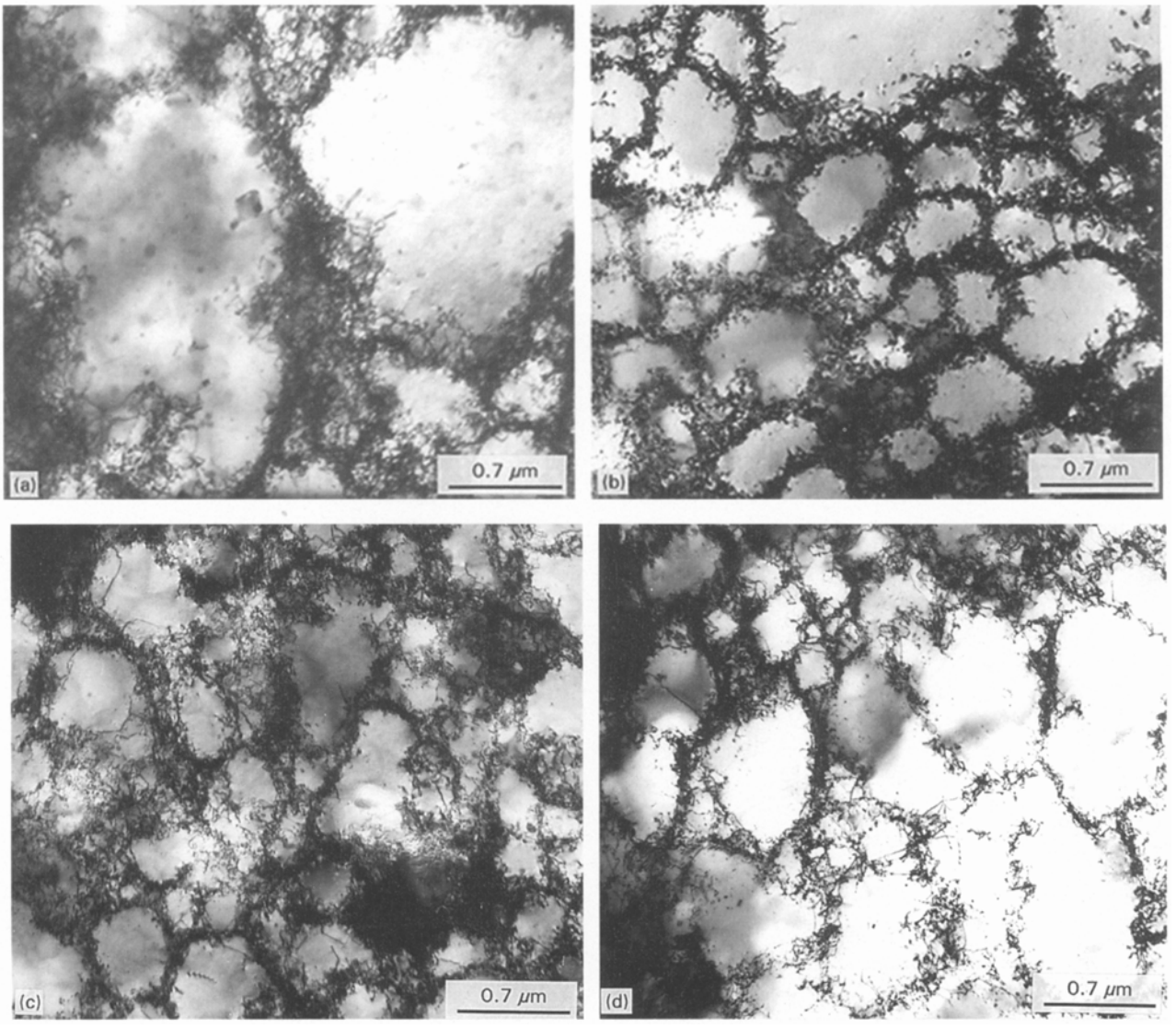

Figure 7 Micrographs showing the comparison of the microstructures for 34 μm grain size for a total of 40% strain at four strain rates: (a) 0.01, (b) 0.05, (c) 0.25 and (d) 2.5 min^{-1}.

grain sizes. The production of larger cells in larger grain-size samples and vice versa can be easily recognized in this figure.

The cell sizes have been measured under different conditions of deformation in this study. Fig. 4 shows the variation in cell sizes as a function of per cent strain for four grain sizes and strain rates used in this study. The curves for larger grain sizes in this figure lie above those of smaller grain sizes, except for the case of 86 μm. The discrepancy in the case of 86 μm may be attributed to the differences in the evolution of the microstructures and may be seen from Fig. 5. This figure shows representative microstructures for the grain size of 86 μm deformed to 10% strain at a strain rate of 5 min^{-1}. The three micrographs shown in this figure are all from a single foil. Fig. 5b shows that well-developed cells are formed in one grain while only twins have been observed in the adjacent grains. Fig. 5a and c show typical twins and the distribution of dislocations, respectively, at other locations within the same sample. The heterogeneity in the microstructure affecting the flow-stress values has also been reported in the case of aluminium [33] under similar deformation conditions. However, why has it been observed only in the case of 86 μm grain size case is not very well understood by the authors at the present time.

The variation in cell sizes with strain rate for different per cent strains, however, does show a relatively more systematic behaviour as shown in Fig. 6. It can be observed in this figure that for the two smaller grain sizes of 34 and 86 μm, though not consistent for all strains, the cell size decreases initially with increase in strain rate and then increases at higher strain rates. This phenomenon was also observed for nickel [34]. A contrasting nature was observed in the case of larger grain size, wherein the cell size increases initially and then decreases at higher strain rates. This contrasting nature was also observed for aluminium [33]. The effect of strain rate on the cell size at a constant strain during room-temperature tensile testing appears to have a dual nature, corresponding to the trends exhibited by aluminium and nickel.

Figs 7 and 8 are the microstructures developed at various strain rates after 40% strain in copper for grain sizes of 34 μm (for the smaller grain size described above) and 105 μm (for the larger grain size).

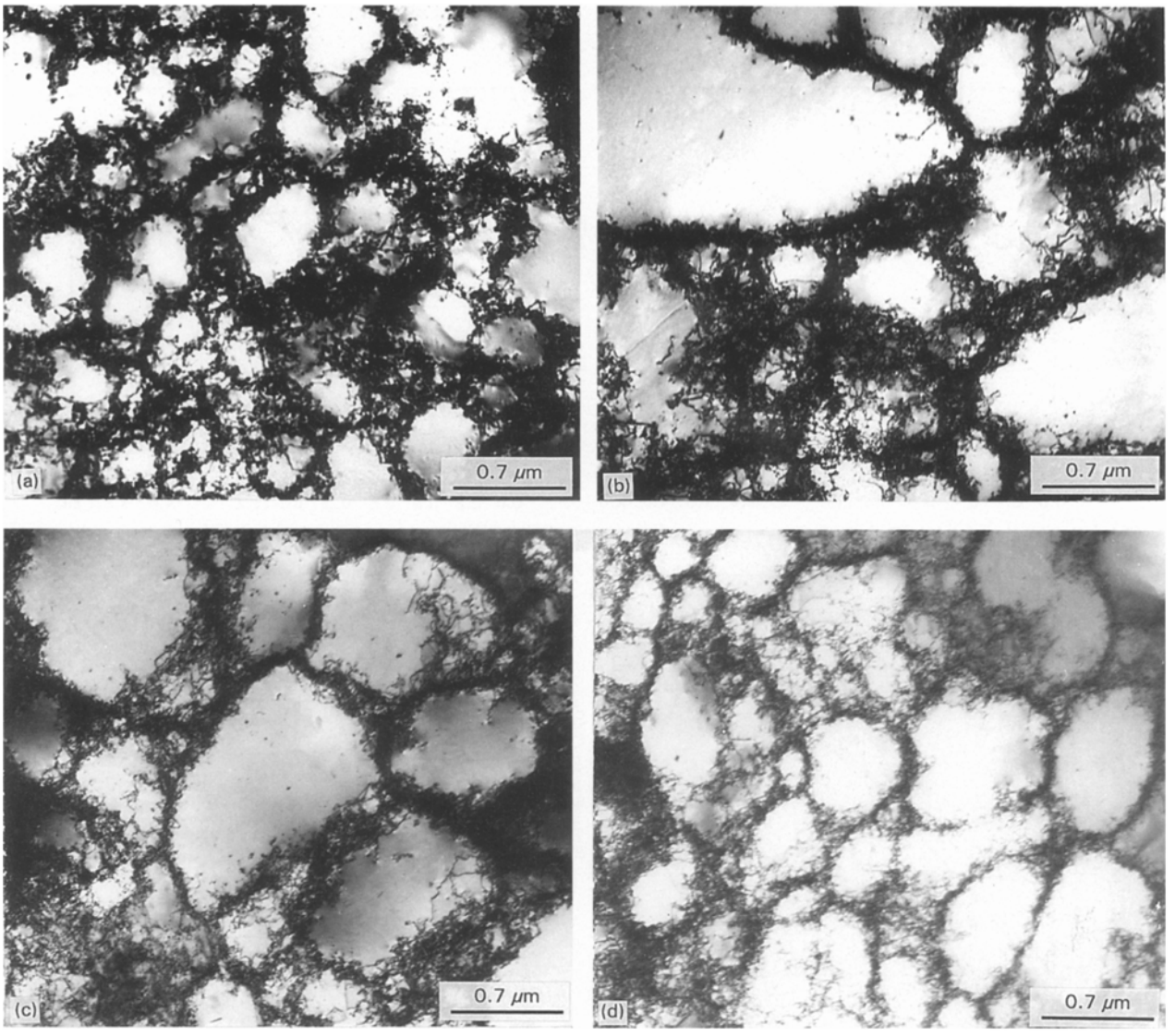

Figure 8 Micrographs showing the comparison of the microstructures for 105 μm grain size for a total of 40% strain at four strain rates: (a) 0.01, (b) 0.05, (c) 0.25 and (d) 2.5 min^{-1}.

The trends described in the previous paragraphs are well documented by the microstructures shown in the two figures. However, surprisingly the sharpening of the cell boundaries with increase in strain rates exhibited by both aluminium and nickel has not been observed in copper. The stacking fault energy (SFE) has been shown to be an important factor for the sharpness of the boundaries developed in the metals, in the sense that higher SFE metals (e.g. aluminium) generally produce sharp boundaries compared to lower SFE metals (e.g. copper and nickel). It appears that the strain-rate effects do not cause any major redistribution of dislocations in the cell walls as the strain increases in copper.

Fig. 9 shows the variation of flow stress, σ, with the inverse of the cell diameter, d (the two are related to each other with the help of a modified Hall–Petch (MHP), Equation 3: $\sigma = \sigma_0 + kd^{-1}$, where σ_0 and k are materials constants). Each graph is plotted for a particular strain rate and different grain sizes. Although the graphs indicate that the MHP equation can be used to relate the flow stress to the cell diameter, it can be noted that there is no consistent relationship between the grain size, cell size and strain rate that can be derived from this figure. Poor fits of the curves can be attributed, in part, to the extensive inhomogeneities in the microstructure and an example of this has been discussed previously in this paper. Also it must be noted that for similar cell sizes, considerable differences in the flow stresses can be present in copper, as was pointed out for aluminium [33]. Similar cell sizes can be obtained by the various combinations of the per cent strain, grain size and strain rate and thus the character of the boundary does not necessarily have to be similar also. An example of this was given in the case of aluminium [33] where penetrability of the boundaries may not be a unique function of these three parameters.

Important information that can be obtained from Fig. 9 is the slope, k, of the straight lines. This gives an estimate of the cell-size strengthening. An attempt has been made to determine the relationship between the constant k, grain size and strain rate as shown in Fig. 10. The results may be interpreted in two different ways: (a) a least square fit curve may be drawn for each grain size, or (b) the data points can simply be interpolated. No consistent behaviour has been found by taking the first approach. The second approach of interpolation of the data points does provide a trend which can be based on small or large grain-size values. At smaller grain sizes (34 and 86 μm), k initially increases, decreases, and then finally increases again, as

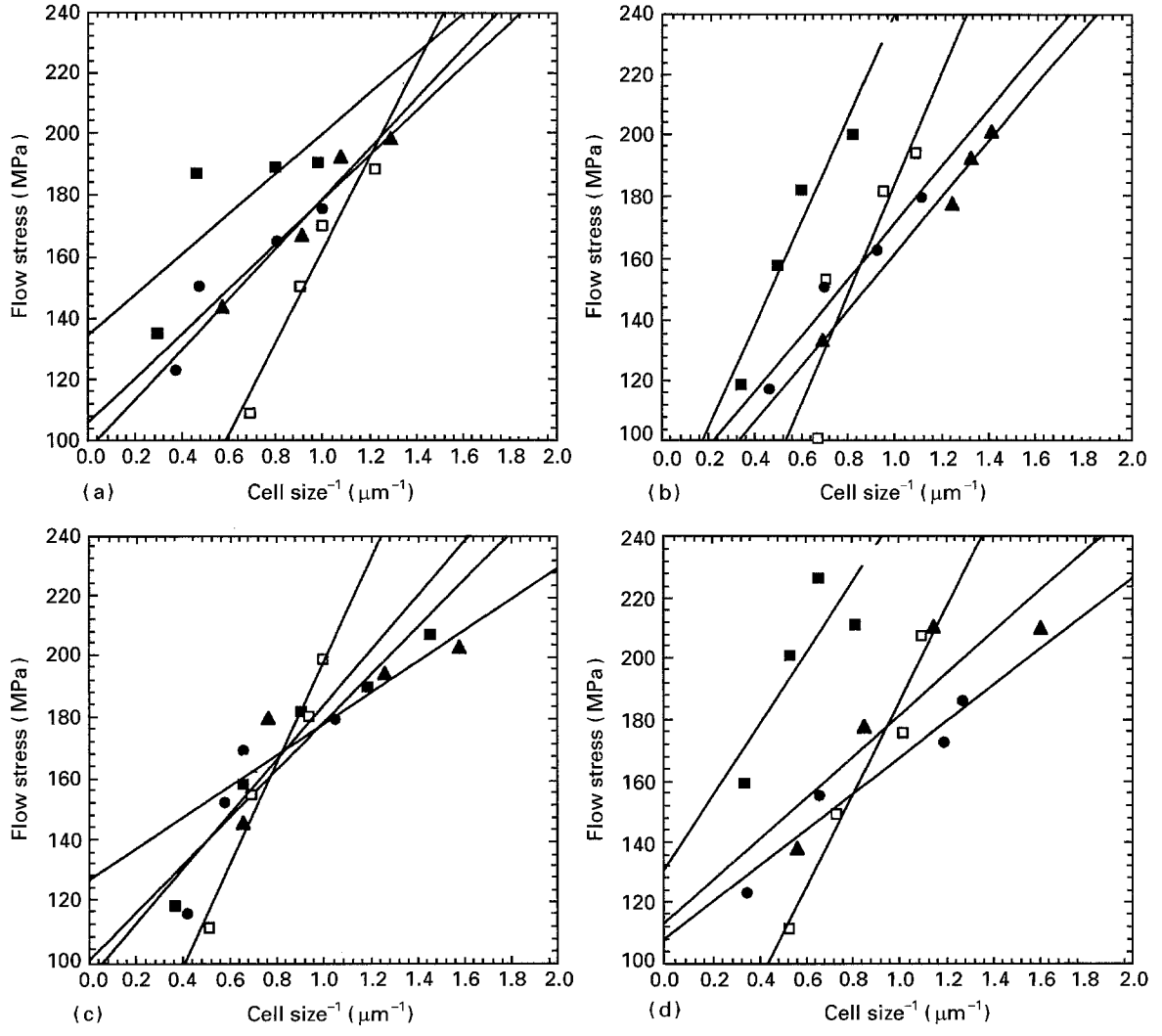

Figure 9 Variation of flow stress as a function of the inverse of the cell size for four different grain sizes of (▲) 34, (■) 86, (□) 105 and (●) 128 μm at strain rates of (a) 0.01, (b) 0.05, (c) 0.25 and (d) 2.5 min^{-1}.

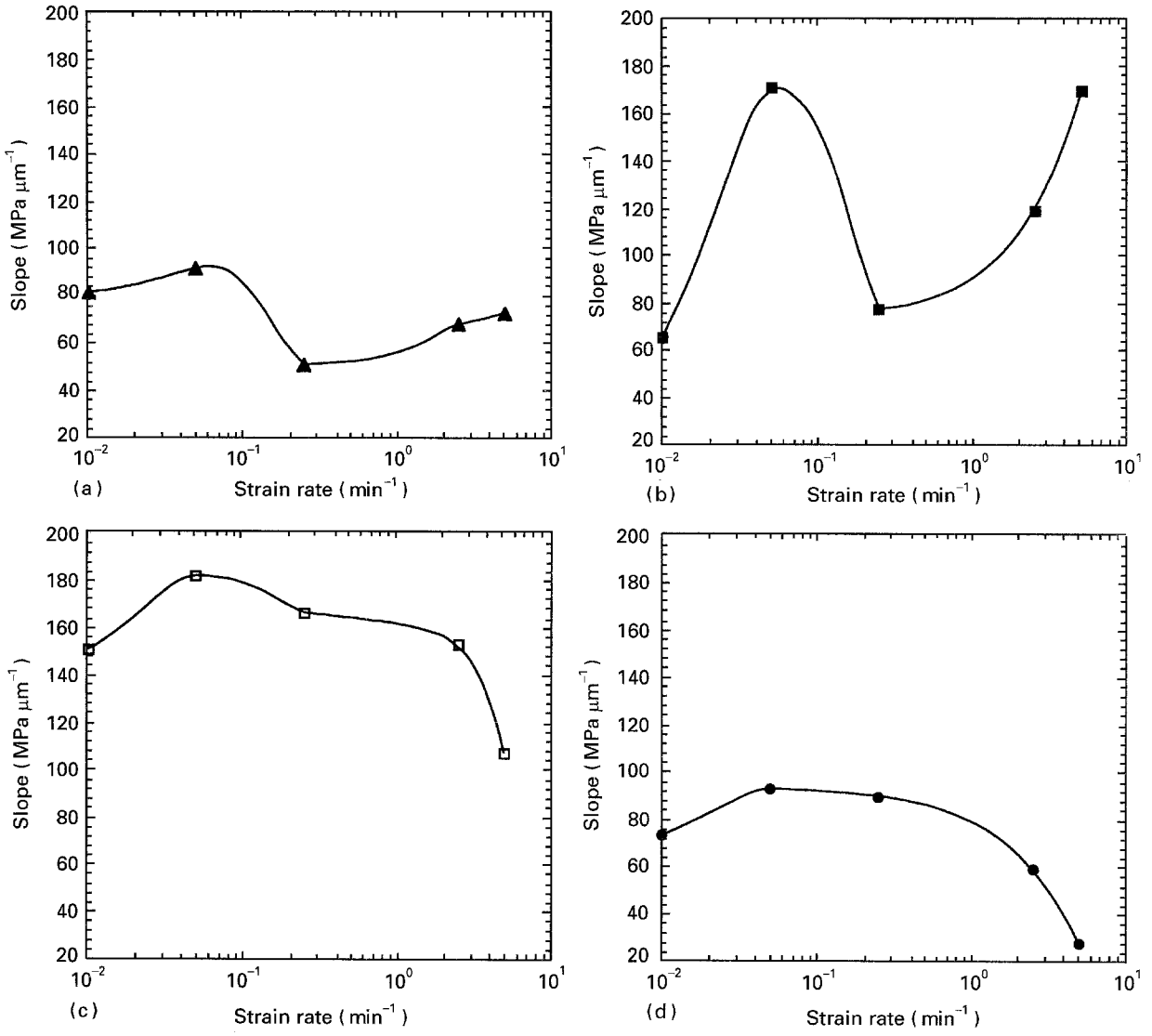

Figure 10 Variation of the slope, k, of modified Hall-Petch plot (from Fig. 9) as a function of strain rate for four grain sizes of (a) 34, (b) 86, (c) 105 and (d) 128 μm.

the strain rate increases, while for large grain sizes (105 and 128 μm) the graphs show only an initial increase, and then a decrease, in k as a function of strain rate. This must, however, be compared with the similar graphs drawn for aluminium and nickel [33,34] where it was shown that k remains constant (though higher values of k were observed for smaller grain sizes) up to a certain strain rate and then increases quite sharply at higher strain-rate values. Work is presently being conducted to investigate the mechanisms assocaited with the figures, such as Fig. 10, in copper and similar graphs for aluminium and nickel.

Acknowledgement

The authors acknowledge the financial support of the Texas Higher Education Coordinating Board for this research through the grant number 003661–018.

References

1. D. L. HOLT, *J. Appl. Phys.* **41** (1970) 3197.
2. J. D. EMBURY, A. S. KEH and R. M. FISHER, *Trans. TMS-AIME* **236** (1966) 640.
3. F. CHEVEL and L. PRIESTER, *Scripta Metall.* **23** (1989) 1871.
4. D. KUHLMANN-WILSDORF, *Mater. Sci. Eng.* **A113** (1989) 1.
5. A. S. MALIN and M. HEATHERLY, *Metal Sci.* (1979) 463.
6. M. R. STAKER and D. L. HOLT, *Acta Metall.* **20** (1972) 569.
7. U. F. KOCKS and H. MECKING, *ibid.* **29** (1981) 1865.
8. D. KNOESON and S. KRITZINGER, *South African J. Phys.* **5** (1982) 19.
9. Y. LAN, H. J. KLAAR and W. DAHL, *Metall. Trans.* **23A** (1992) 537.
10. K. R. CARSON and J. WEERTMAN, *Trans. Metall. Soc. AIME* **242** (1968) 1413.
11. N. HANSEN, *Mater. Sci. Technol.* **6** (1990) 1039
12. N. K. PARK and B. A. PARKER, *Mater. Sci. Eng.* **A113** (1989) 431.
13. W. D. NIX and D. A. HUGHES, *ibid* **A122** (1989) 153.
14. D. J. HENSEN and N. HANSEN, *Acta Metall.* **38** (1990) 1369.
15. C. TOME, G. R. CANOVA, U. F. KOCKS, J. J. JONAS and N. CHRISTODOULOU, *ibid* **32** (1984) 1637.
16. V. S. ANANTHAN, T. LEFFERS and N. HANSEN, *Scripta Metall. Mater.* **25** (1991) 137.
17. A. W. THOMPSON, M. I. BASKES and W. F. FLANAGAN, *Acta Metall.* **21** (1973) 1017.
18. A. W. THOMPSON, *Metall. Trans.* **8A** (1977) 833.
19. D. J. PARRY and A. G. WALKER, "International Conference on Mechanical Properties of Materials at High Strain Rates" (Institute of Physics, Oxford, 1984 pp. 329–36.

20. S. MEHTA and S. K. VARMA, *J. Mater. Sci.* **27** (1992) 3570.
21. H. FUGITA and T. TABATA, *Acta Metall.* **21** (1973) 355.
22. J. J. GRACIO and J. V. FERNANDES *Mater. Sci. Eng.* **A118** (1987) 97.
23. W. H. GOURDIN and D. H. LASSILA, *Acta Metall.* **39** (1991) 2337.
24. D. J. DINGLEY and D. McLEAN, *ibid.* **25** (1977) 885.
25. A. W. THOMPSON, *ibid.* **25** (1977) 83.
26. E. P. ABRAHAMSON "Surfaces and interfaces" (University Press, Syracuse, NY, 1968) pp. 262–9.
27. A. KORBEL and K. SWIATKOWSKI, *J. Met. Sci.* **6** (1972) 60.
28. S. THIAGARAJAN and S. K. VARMA, *Metall. Trans.* **22A** (1990) 258
29. S. THIAGARAJAN, A. GUREVITCH, L. E. MURR, S. K. VARMA, W. W. FISHER and A. ADVANI, in "Modeling the deformation of crystalline solids", edited by T. C. Lowe, A. D. Rollett, P. S. Follansbee and G. S. Daehn (Minerals, Metals and Materials Society, Warrendale, PA, 1991) pp. 159–71.
30. A. GUREVTICH, L. E. MURR, S. K. VARMA, S. THIAGARAJAN and W. W. FISHER, in "Shock-wave and high-strain-rate phenomena in materials", edited by M. A. Meyers, L. E. Murr and K. P. Staudhammer (Marcel Dekker, New York, NY, 1992) pp. 521–8.
31. S. THIAGARAJAN and S. K. VARMA, *J. Mater. Sci. lett.* **11** (1992) 692.
32. D. SIL, J. G. RAO and S. K. VARMA, *Metall. Trans.* **23A** (1992) 3166.
33. D. SIL and S. K. VARMA, *ibid.* **24A** (1993) 1153.
34. J. G. RAO and S. K. VARMA, *ibid.* **24A** (1993) 2559.
35. L. E. MURR and D. KUHLMANN-WILSDORF, *Acta Metall.* **26** (1978) 847.
36. S. K. VARMA, J. KALYANAM, L. E. MURR and V. SRINIVAS, *J. Mater. Sci. Lett.* **13** (1994) 107.

Received 15 June 1994
and accepted 20 January 1995